Applied Physics B (2024) 130:130
https://doi.org/10.1007/s00340-024-08264-3

Applied Physics B
Lasers and Optics

RESEARCH

Enhanced THz generation by Hermite-cosh-Gaussian chirped laser in static magnetized plasma

Hitesh Kumar Midha[1] · Vivek Sharma[1] · Niti Kant[2] · Vishal Thakur[1]

Received: 12 October 2023 / Accepted: 17 June 2024 / Published online: 28 June 2024

Abstract

The investigation of tuneable and energy-efficient terahertz (THz) generation has become a prominent field of study due to its significant ramifications in various disciplines, including chemical analysis and medical research. This study selects two co-propagating Hermite-cosh-Gaussian (HchG) laser beams with positively chirped frequencies for analysis. The laser beam exhibits interaction with a collisionless underdense plasma in the presence of a static transverse magnetic field. The interaction between laser and plasma exhibits nonlinear characteristics, leading to the creation of THz radiation with high energy efficiency. The primary objective of this study is to conduct an analytical examination of the correlation between THz conversion efficiency, normalised transverse distance, and plasma frequency. Additionally, the analysis will consider various laser parameters, including the Hermite polynomial mode index (s), decentred parameter (a), and frequency chirp (b). The results show that in off-resonant condition THz conversion efficiency quickly decreases and approaches to zero for normalised THz frequencies. The observed phenomenon entails an augmentation in the normalized amplitude of terahertz (THz) waves, accompanied by a displacement of the peak towards greater normalized transverse distance values. This occurrence is contingent upon the variation of the Hermite polynomial mode index within the range of 0 *to* 2. As the chirp parameter (b) is increased from 0.0011 *to* 0.0099, the normalised terahertz (THz) amplitude exhibits an increase with respect to the normalised transverse distance for values of *s* equal to 0,1 *and* 2. The proposed methodology demonstrates significant use in generating high-intensity, adjustable, and energy-efficient terahertz (THz) radiation sources through the manipulation of the decentred parameter and Hermite polynomial mode index values.

1 Introduction

Terahertz wave applications in the fields of chemical analysis, non-destructive testing, medical imaging and research is gaining attention of scholars and industries [1–4]. A wide variety of fields such as nonlinear optics, harmonic generation, self-focusing, filamentation, electron acceleration, wake field generation, terahertz wave generation, etc. uses the laser plasma interaction process [5–10]. Hermite-cosh-Gaussian beam is the member of Hermite sinusoidal Gaussian family. The Hermite-cosh-Gaussian function is utilized to represent a laser beam profile that encompasses Hermite polynomials, Gaussian and hyperbolic cosine components, and Gaussian-like spatial variation. The Hermite-cosh-Gaussian function's paraxial wave solution is introduced by Casperson and Tovar [11]. Through the use of a paraxial wave solution, Belafhal et al. [12] theoretically examined the wave propagation characteristics of the Hermite-cosh-Gaussian function in the ABCD system.

Researchers investigate the Hermite-cosh-Gaussian laser beam in diverse laser plasma interaction process. The Hermite-cosh-Gaussian laser beam in magneto-active plasma was studied by Patil et al. [13]. They investigated the role of decentred parameter and the mode index on self-focusing. The self-focusing of a Hermite-cosh-Gaussian laser beam in ramp density and under density plasma profiles was investigated by Nanda et al. [14, 15]. The Hermite-cosh-Gaussian laser beam in ripple density plasma was studied numerically by Kaur et al. [16]. In semiconductor plasma, Wani et al. [17] looked at the self-focusing of a Hermite-cosh-Gaussian beam. The third harmonics generation by Hermite-cosh-Gaussian beam in the presence of wiggler magnetic field was theoretically investigated by Sharma et al. [18]. The beat

✉ Vishal Thakur
vishal20india@yahoo.co.in

[1] Department of Physics, Lovely Professional University, G.T. Road, Phagwara, Punjab 144411, India

[2] Department of Physics, University of Allahabad, Allahabad, Uttar Pradesh, India

wave of Hermite-cosh-Gaussian laser beam absorption in collisional nano cluster plasma profile was studied by Verma et al. [19]. In this research, they looked at the Bernstein wave parameters. In collisional plasma, the second harmonics generation of the Hermite Gaussian beam was explored by Wadhwa et al. [20]. The researchers conducted an investigation on the influence of mode indices on the generation of harmonics and the phenomenon of self-focusing. In order to generate terahertz waves, Hamster et al. [21] investigate the interaction between a short, powerful laser pulse and plasma. The researchers conducted an investigation on the nonlinear ponderomotive force effect in the production of terahertz waves. In their study, Safari et al. [22] investigated the properties of collisional plasma by employing laser beams with Gaussian and Hermite-cosh-Gaussian profiles. They came to the conclusion that plasma and laser parameters are crucial for terahertz field amplitude. The terahertz wave generation with radially polarized Hermite-cosh-Gaussian laser beam in hot collisional plasma was studied by Chaudhary et al. [23]. In their theoretical inquiry, Malik et al. [24] looked at the creation of terahertz waves using two Hermite-cosh-Gaussian laser beams in a periodically varying plasma density profile with an applied magnetic field. They investigated how terahertz wave production was affected by the decentred parameter, Hermite function order, and applied magnetic field. Hashemzadeh [25] looked into the production of terahertz waves in magnetized plasma using laser beams that were Hermite-cosh-Gaussian and hollow Gaussian. In their study, Sharma et al. [26] examined the phenomenon of second harmonic generation in a wiggler magnetized plasma by employing a cosh-Gaussian laser beam. In collisional inhomogeneous plasma, Safari et al. [27] looked at the nonlinear processes of Hermite-cosh-Gaussian and Laguerre-Gaussian beam interaction. For the greatest electric field amplitude at terahertz frequencies, they examined various laser parameters and density ripple. The Hermite-cosh-Gaussian laser pulse is investigated by Rajput et al. [28] in their work on electron acceleration in a vacuum. The researchers utilized laser pulses with both circular and linear polarization. The terahertz production was investigated by Mehta et al. [29, 30] by the utilization of a transverse external magnetic field in conjunction with underdense plasma and chirped laser pulses. The authors of the study illustrate the enhancement of the terahertz electric field in the presence of a magnetic field, as well as the optimization of the chirp value. They also investigate the impact of chirped laser pulses on the ripple in density.

Wu et al. [31] studied the chirped laser pulse-induced terahertz pulse production in a lithium niobate crystal at ambient temperature. They produce a 0.2 mJ terahertz pulse for their research. Jiang et al. [32] generated 0.3 mW terahertz pulses while studying the GaP crystal using a negatively chirped femtosecond laser pulse. In order to generate terahertz waves at beat frequency, Gurjar et al. [33] looked at the nonlinear interaction of chirped laser pulse interaction with slanting plasma modulation. They demonstrate that the generated terahertz wave amplitude is strongly affected by

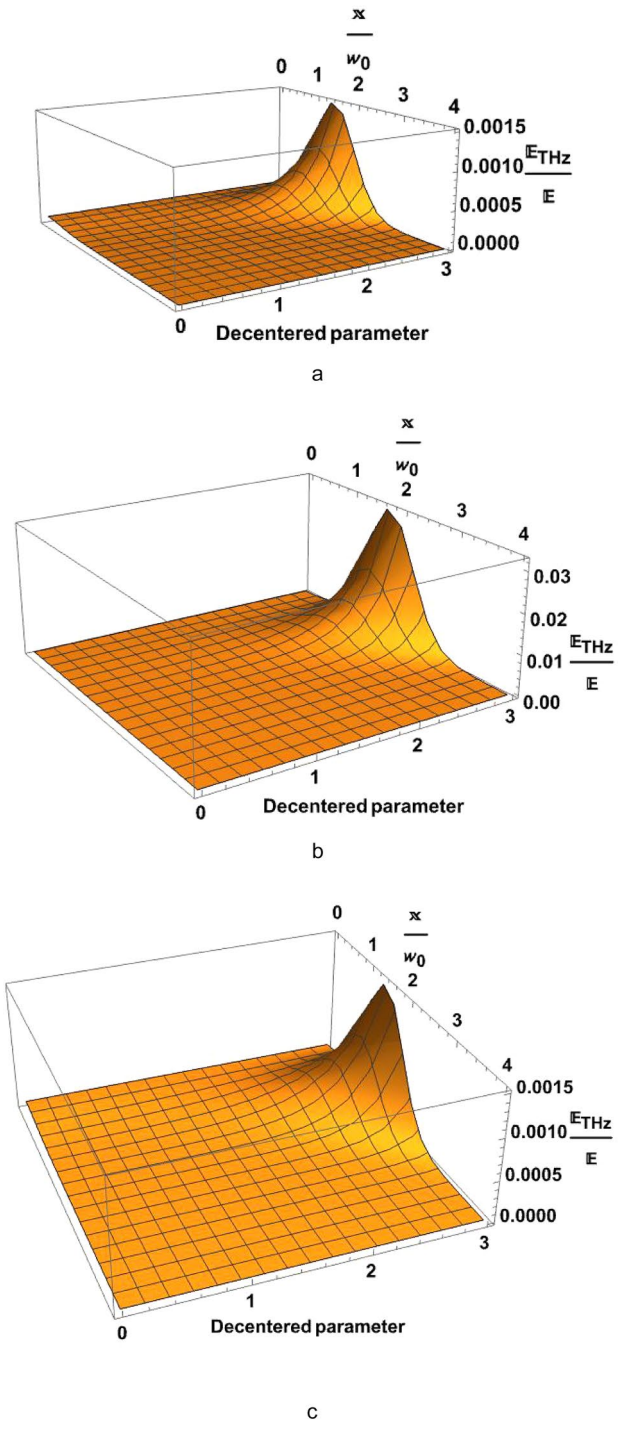

Fig. 1 Variation of normalized THz amplitude with normalized transverse distance and decentered parameter. ($s = 0$, $r = 0.5r_0$, **a**) $s = 0$, **b** s = 1, **c** s = 2. Other parameters are same as mentioned above

the slanting plasma profile. Mehta et al. [29] investigated how frequency chirp affected the generation of THz waves in magneto-active plasma. Scientists and researchers investigate several phenomena related to the interaction between lasers and plasma [34–43].

In the current study, two linearly polarized chirped Hermite-cosh-Gaussian beams are propagating in z direction. These laser beams propagated in underdense plasma with externally applied transverse static magnetic field. The interaction between laser and plasma results in the generation of intense terahertz (THz) waves. Tuneable efficient THz radiation source can be achieved by adjusting the laser and plasma parameters. Section 2 of this study encompasses the analytical derivation of the ponderomotive force, equation of motion, nonlinear plasma current density, and subsequently, the creation of THz fields. Section 3 of this paper examines the relationship between the normalized THz electric field and several factors, including the normalized THz frequency, normalized transverse distance, and chirp parameter. In Sect. 4, we draw the Conclusions. The document concludes with the inclusion of references.

2 Analytical study of THz generation

Two waves, which are linearly polarized and have the Hermite-cosh-Gaussian profile, are propagating in the z direction. The direction of polarization of the electric field is aligned with the x-axis, and can be mathematically expressed by the following equation.

$$\vec{E}_J = \hat{x}E_0 H_s\left(\frac{\sqrt{2}x}{w_0}\right)\cosh\left(\frac{ax}{w_0}\right)e^{-\left(\frac{x^2}{w_0^2}\right)}e^{i(k_J z-\omega_J t)} \quad \text{where,} \quad J=1,2 \tag{1}$$

In this context, E_0 represents the amplitude of the laser beam, w_0 denotes the beam waist, a signifies the decentred parameter of the cosh profile, and s represents the mode index of the Hermite polynomial H_s.

Corresponding magnetic field of laser beam are

$$\vec{B}_j = \frac{\vec{k_J}\times\vec{E}_j}{\omega_J} \quad \text{where,} \quad J=1,2 \tag{2}$$

Incident laser beam is positively chirped and chirp is represented as $\omega_1 = \omega_0 + b\omega_0^2\left(t-\frac{z}{c}\right)$, where, ω_0 is the frequency of incident laser beam in the absence of chirp, b is chirp parameter, c is velocity of light. We choose ω_2 such as $\omega_1 - \omega_2 = \omega$ lies in THz range.

So

$$\omega_2 = \omega_1 - \omega = \left\{\omega_0 + b\omega_0^2\left(t-\frac{z}{c}\right)\right\} - \omega \tag{3}$$

An external static magnetic field is applied along the y-axis i.e. $B_s = B_0\hat{y}$.

Here, B_0 is the amplitude of static magnetic field.

During the initial stage, it can be assumed that electrons are in a state of rest, resulting in the absence of any magnetic force acting upon them. The oscillatory velocity of a plasma electron can be determined by using the equation of motion $m\left(d\overrightarrow{V_J}/dt\right) = -e\overrightarrow{E_J} - m\overrightarrow{V_J}\nu$.

By solving this equation, we get.

$$\overrightarrow{V_1} = \frac{e\overrightarrow{E_1}}{im\omega_0\left\{1+b\omega_0\left(2t-\frac{z}{c}\right)\right\} - m\nu} \tag{4}$$

$$\overrightarrow{V_2} = \frac{e\overrightarrow{E_2}}{im\omega_0\left\{1+b\omega_0\left(2t-\frac{z}{c}\right)-\frac{\omega}{\omega_0}\right\} - m\nu} \tag{5}$$

here, e, m, ν is charge, rest mass and collisional frequency of the plasma electron respectively.

This oscillatory velocity of plasma electron give rise to nonlinear ponderomotive force.

Nonlinear ponderomotive force is

$$\overrightarrow{F_P}^{NL} = -\frac{e}{2c}\left(\overrightarrow{V_1}\times\overrightarrow{B_2}^* + \overrightarrow{V_2}^*\times\overrightarrow{B_1}\right) - \frac{m}{2}\vec{\nabla}\left(\overrightarrow{V_1}\overrightarrow{V_2}^*\right) \tag{6}$$

here, * represents the complex conjugate.

Solving this equation by putting values of $\overrightarrow{V_1}, \overrightarrow{V_2}^*, \overrightarrow{B_1}$, and $\overrightarrow{B_2}^*$, we get

$$\overrightarrow{F_P}^{NL} = -\hat{z}\frac{e^2E_1E_2^*}{2im\omega_0 c}\left(\frac{2\frac{\nu}{\omega_0}-\frac{\omega}{\omega_0}}{\left\{1+b\omega_0\left(2t-\frac{z}{c}\right)-\frac{\nu}{i\omega_0}\right\}\left\{1+b\omega_0\left(2t-\frac{z}{c}\right)-\frac{\omega}{\omega_0}+\frac{\nu}{i\omega_0}\right\}}\right) - \hat{z}$$
$$\frac{be^2E_1E_2^*}{m\omega_0 c}\left(\frac{\left\{1+b\omega_0\left(2t-\frac{z}{c}\right)-\frac{\omega}{2\omega_0}\right\}}{\left\{\left\{1+b\omega_0\left(2t-\frac{z}{c}\right)\right\}-\frac{\nu}{i\omega_0}\right\}^2\left\{1+b\omega_0\left(2t-\frac{z}{c}\right)-\frac{\omega}{\omega_0}+\frac{\nu}{i\omega_0}\right\}^2}\right) \tag{7}$$

Plasma electrons starts moving in circular path due to Lorentz force by external static magnetic field. Circular motion of plasma electron interacts with electric field of laser beam result into angular motion of plasma electron with cyclotron frequency ω_c.

By solving the equation of motion $\partial\vec{V}_{\omega}^{NL}/\partial t = \vec{F}_P^{NL}/m - \nu_{en}\vec{V}_{\omega}^{NL} - e\left\{\vec{V}_{\omega}^{NL}\times\vec{B}\right\}/(mc)$, we get the oscillatory velocity of plasma electron such as

$$\overrightarrow{V_{\omega}^{NL}} = \frac{\omega_c\hat{x} - i\omega\hat{z}}{m\left(\omega_c^2 - \omega^2\right)}F_P^{NL} \tag{8}$$

here, we consider $\omega_{1,}\omega_2 >> \omega_c, \omega_P$.

Where, $\omega_P$is plasma frequency is such as $\omega_P^2 = 4\pi ne^2/m$ and $\omega_c = eB_0/mc$ is cyclotron frequency. Nonlinear oscillatory current density can be calculated by solving this equation

$$\vec{J}^{NL} = -\frac{1}{2}ne\vec{V}^{NL}, \Rightarrow \vec{J}^{NL} = -\frac{\omega_P^2}{8\pi e}\frac{\omega_c\hat{x} - i\omega\hat{z}}{\left(\omega_c^2 - \omega^2\right)}F_{Pz}^{NL} \tag{9}$$

This nonlinear current density is responsible for THz generation. By using III and IV Maxwell's equation, $\vec{\nabla}\times\vec{E} = -\frac{1}{c}\left(\partial\vec{B}/\partial t\right)$ and $\vec{\nabla}\times\vec{B} = (\varepsilon/c)\left(\partial\vec{E}/\partial t\right) + (4\pi/c)\vec{J}^{NL}$, we can calculate the THz wave generation equation.

Equation for THz generation is

$$\vec{\nabla}.\left(\vec{\nabla}\overrightarrow{E_{THz}}\right) - \nabla^2\overrightarrow{E_{THz}} = \frac{\omega^2}{c^2}\varepsilon\overrightarrow{E_{THz}} + \frac{4\pi i\omega}{c^2}\vec{J}^{NL} \tag{10}$$

In order to neglect higher order derivatives due to fast variation of THz field. So

$$E_{THz} = \frac{\omega_P^2}{2e\varepsilon\omega\sqrt{\omega_c^2 - \omega^2}} \left\{-\frac{e^2E_1E_2^*}{2im\omega_0c}\left(\frac{2\frac{\nu}{\omega_0} - \frac{\omega}{\omega_0}}{\left\{1 + b\omega_0\left(2t - \frac{z}{c}\right) - \frac{\nu}{i\omega_0}\right\}\left\{1 + b\omega_0\left(2t - \frac{z}{c}\right) - \frac{\omega}{\omega_0} + \frac{\nu}{i\omega_0}\right\}}\right) - \frac{be^2E_1E_2^*}{m\omega_0c} \left(\frac{\left\{1 + b\omega_0\left(2t - \frac{z}{c}\right) - \frac{\omega}{2\omega_0}\right\}}{\left\{\left\{1 + b\omega_0\left(2t - \frac{z}{c}\right)\right\} - \frac{\nu}{i\omega_0}\right\}^2\left\{1 + b\omega_0\left(2t - \frac{z}{c}\right) - \frac{\omega}{\omega_0} + \frac{\nu}{i\omega_0}\right\}^2}\right)\right\} \tag{11}$$

For collisionless plasma, the Eq. (11) becomes

$$\frac{E_{THz}}{E_0} = \frac{e\omega_P^2}{2e\omega\sqrt{\omega_c^2 - \omega^2}} \frac{\left\{H_s\left(\frac{\sqrt{2}x}{w_0}\right)\cosh\left(\frac{ax}{w_0}\right)\right\}^2 e^{-\left(2x^2/w_0^2\right)}E_0}{m\omega_0c\left\{1 + b\omega_0\left(2t - \frac{z}{c}\right)\right\}\left\{1 + b\omega_0\left(2t - \frac{z}{c}\right) - \frac{\omega}{\omega_0}\right\}} \sqrt{b^2\left(\frac{\left\{1 + b\omega_0\left(2t - \frac{z}{c}\right) - \frac{\omega}{2\omega_0}\right\}}{\left\{1 + b\omega_0\left(2t - \frac{z}{c}\right)\right\}\left\{1 + b\omega_0\left(2t - \frac{z}{c}\right) - \frac{\omega}{\omega_0}\right\}}\right)^2 - \frac{1}{4}\left[\frac{\omega}{\omega_0}\right]^2} \tag{12}$$

3 Result and discussion

In this investigation of THz generation, two Hermite-cosh Gaussian polarised laser beams are positively chirped and propagating in cold collisionless underdense plasma. For this study we choose suitable laser parameter such as femtosecond Ti–Sapphire laser with wave length of 800 nm having angular frequency 2.35×10^{15} rad/sec, chirp parameter of 0.0099, beam waist of 5×10^{-3} cm and electric field amplitude of 5×10^7 V/cm.. Plasma parameters are optimised as plasma density is $9.74 \times 10^{16}\text{cm}^{-3}$, whose corresponding plasma frequency ω_P is1.76×10^{13}Hz. Here in present study we choose $\omega = 1.07\omega_P$ where, $\omega_1, \omega_2 > \omega_P$ and applied external static magnetic field $B_0$is 10×10^4 gauss.

3.1 Effect of normalised transverse distance (x/w_0) and decentred parameter (b)

Variation of normalized THz wave amplitude is calculated at different normalized transverse distance and different decentred values $a = 0, 1, 2, 3$. A three dimensional curve is plotted for different values of Hermite polynomial mode index values $s = 0, 1, 2$ at $E_0 = 5 \times 10^7$ V/cm and external static magnetic field is 10×10^4 gauss (Fig. 1).

When the Hermite polynomial mode index value is varied for $s = 0, 1$ and 2, the normalized transverse distance and normalised THz amplitude exhibit a shift towards higher values, specifically from 1.4 to 1.9 and from 0.0015 to 0.8, respectively. The findings of this study indicate a significant rise in normalised terahertz (THz) amplitude when the decentred parameter exceeds a value of 2.

3.2 Effect of normalised THz frequency (ω/ω_P)

This study aims to conduct a theoretical analysis of the relationship between the normalised amplitude of THz radiation and the normalised frequency of THz waves (Fig. 2). The analysis focuses on various values of the Hermite polynomial mode index, specifically $s = 0, 1, 2$ and different decentered parameter values $a = 0, 1, 2$.

The normalized terahertz amplitude with the Hermite polynomial mode with index $s = 0, 1, 2$ rises when the chirp parameter b is set to 0.0099 and a static magnetic field of 10×10^4 gauss is applied. In the case of larger values of normalised THz frequency, it can be observed that the normalised THz amplitude experiences a rapid decline and eventually approaches zero when the frequency exceeds 1.2 times the normalised plasma frequency ($\omega > 1.2\,\omega_P$). There is a lack of substantial impact

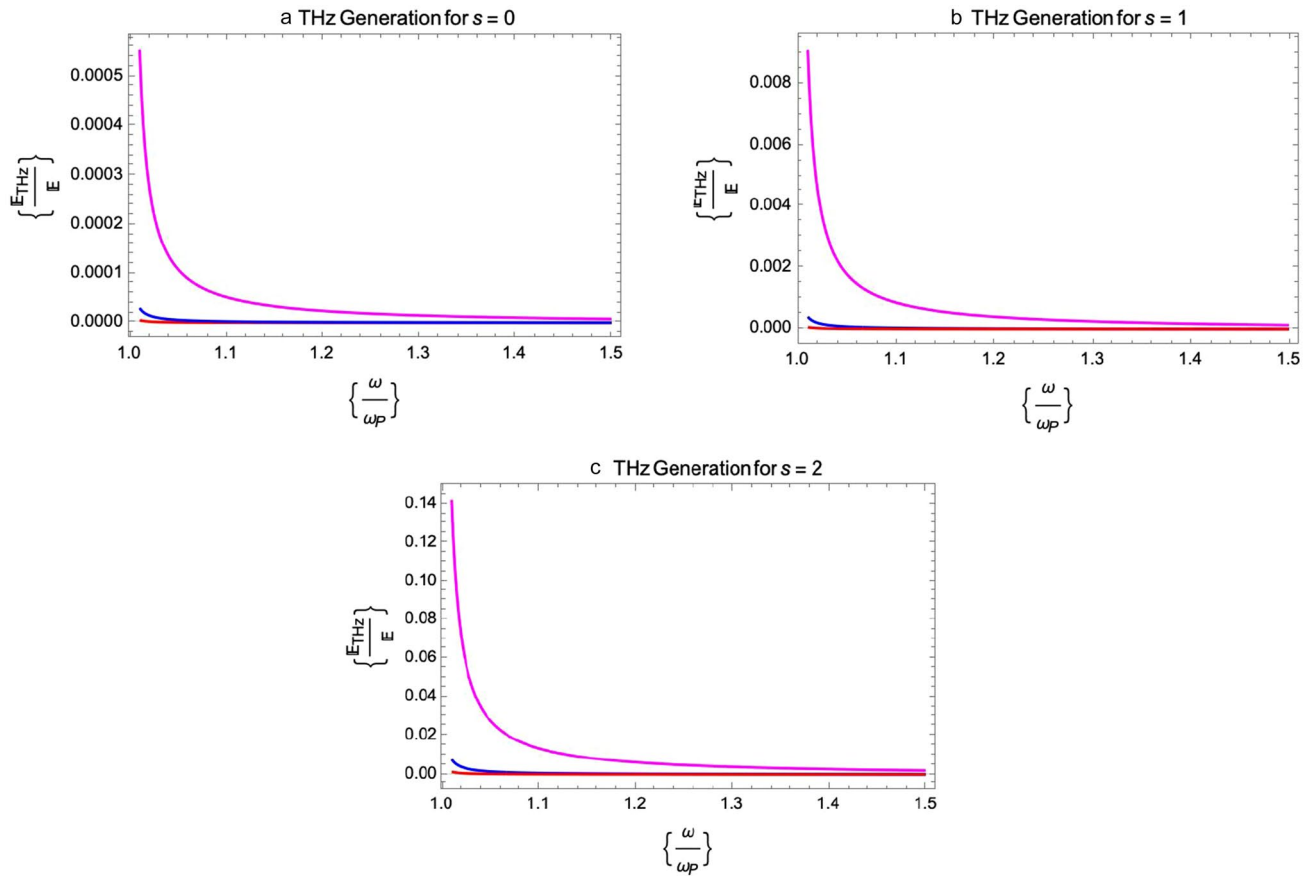

Fig. 2 Variation of normalized THz amplitude with normalized THz frequency with mode index **a** $s = 0$, $r = 0.5\, r_0$, s $= 0$, **b**$s = 1$, **c**$s = 2$ are shown. For decentered parameter $a = 0$(red), a = 1(blue)and a = 2(magenta)for chirp parameter b = 0.0099. Other parameters are same as mentioned above

observed when considering the decentred parameter and chirp parameter beyond the specified threshold.

3.3 Effect of chirp parameter (b)

This study focuses on examining the relationship between the normalised THz amplitude and the normalised THz frequency. The examination explores various values of the Hermite polynomial mode index ($s = 0, 1, 2$) and the decentred parameter value ($a = 2$) under varied chirp levels b = 0.0011, 0.0044, 0.0066 and 0.0099 (Fig. 3).

As the Hermite polynomial mode index value is incremented from 0 to 2, there is an observed increase in the normalised THz amplitude, ranging from around 0.0016 to 0.26 and there is a noticeable shift in the peak towards larger normalized transverse distance values from 0.92 to 1.63. The THz normalized amplitude exhibits an increasing trend as the chirp parameter (b) varies across multiple values, specifically 0.0011, 0.0044, 0.0066 and 0.0099.

The results of this investigation align with the findings reported by Choudhary et al. [23]. The researchers reached the conclusion that the utilization of the Hermite-cosh-Gaussian beam is an effective method for generating terahertz (THz) radiation. In the course of our inquiry, we employed a chirped Hermite-cosh-Gaussian beam as a means to generate terahertz (THz) waves.

4 Conclusion

This study examines the propagation of two Hermite-cosh-Gaussian chirped laser beams in a collisionless underdense plasma medium. An analytical solution is derived to determine the efficiency of terahertz (THz) generation, considering various characteristics such as the normalized THz frequency, normalized transverse distance, and frequency chirp. The resulting solution is then analysed to optimize these parameters, aiming to achieve a tuneable and energy-efficient THz source. The normalized THz amplitude exhibits

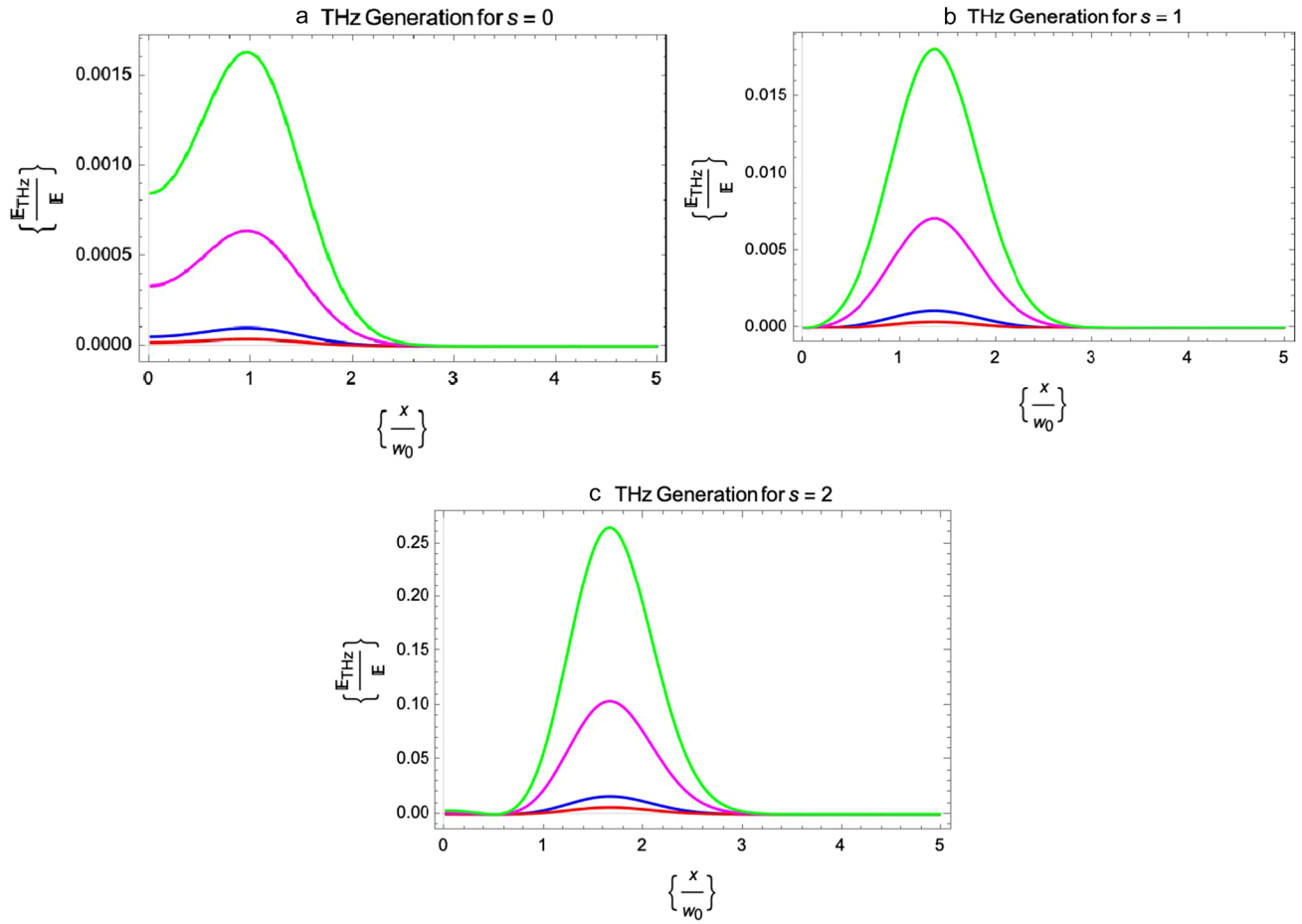

Fig. 3 Variation of normalized THz amplitude with normalized transverse distance with mode index **a** $s = 0$, $r = 0.5\ r_0$, s = 0, **b** s = 1, **c** s = 2 are shown. For b = 0.0011(red), b = 0.0044(blue), b = 0.0066 (magenta), b = 0.0099(green) for decentered parameter a = 2. Other parameters are same as mentioned above

significant values up to 0.8 for normalized transverse distances corresponding to s values of 0, 1, and 2. The findings indicate that as the index value of the Hermite polynomial mode increases from 0 to 2, there is a discernible rise in the normalized amplitude of the THz signal. Additionally, there is an observable displacement of the peak towards higher values of normalized transverse distance.

Author contributions Hitesh Kumar Midha: derivation, methodology, analytical modelling, and graph plotting; Vivek Sharma: numerical analysis; Niti Kant: numerical analysis and result discussion; Vishal Thakur: supervision, reviewing, and editing.

Funding Not applicable.

Data availability The data that support the findings of this study are available from the corresponding authors upon reasonable request.

Declarations

Conflict of interest The authors declare no competing interest.

Ethical approval Not applicable.

Consent to participate Not applicable.

Consent for publication Not applicable.

References

1. Y. Ueno, A. Katsuhiro, Analytical terahertz spectroscopy. Anal. Sci. **24**(2), 185–192 (2008)

2. Y.H. Tao, J.F. Anthony, P. Vincent, Non-contact, non-destructive testing in various industrial sectors with terahertz technology. Sensors **20**(3), 712 (2020)
3. A.J. Fitzgerald, An introduction to medical imaging with coherent terahertz frequency radiation. Phys. Med. Biol. **47**(7), R67 (2002)
4. P.H. Siegel, Terahertz technology in biology and medicine. IEEE Trans. Microw. Theory Tech.Microw. Theory Tech. **52**(10), 2438–2447 (2004)
5. S. Kumar, S. Vij, N. Kant, V. Thakur, Resonant excitation of THz radiations by the interaction of amplitude-modulated laser beams with an anharmonic CNTs in the presence of static DC electric and magnetic fields. Chin. J. Phys. **78**, 453–462 (2022)
6. V. Thakur, N. Kant, Stronger self-focusing of cosh-Gaussian laser beam under exponential density ramp in plasma with linear absorption. Optik **183**, 912–917 (2019)
7. V. Thakur, N. Kant, Resonant second harmonic generation by a chirped laser pulse in a semiconductor. Optik **130**, 525–530 (2017)
8. V. Thakur, N. Kant, S. Vij, "Effect of cross focusing of two laser beams on THz radiation in graphite nanoparticles with density ripple. Phys. Scr. **95**(4), 045602 (2020)
9. S. Vij, N. Kant, V. Thakur, Resonant enhancement of THz radiation through vertically aligned carbon nanotubes array by applying wiggler magnetic field. Plasmonics **14**, 1051 (2019)
10. A. Mehta, N. Kant, Terahertz radiation generation driven by the frequency chirped laser pulse in magneto-active plasma. In: Proc. SPIE 10917, Terahertz, RF, Milimeter, and Sub-milimeter-Wave Technology and Applications 25, 16, 9170R (2019)
11. L.W. Casperson, A. Tovar, Hermite–sinusoidal-Gaussian beams in complex optical systems. JOSA A **15**(4), 954–961 (1998)
12. A. Belafhal, M. Ibnchaikh, Propagation properties of Hermite-cosh-Gaussian laser beams. Opt. Commun.Commun. **186**(4–6), 269–276 (2000)
13. S.D. Patil et al., Focusing of Hermite-cosh-Gaussian laser beams in collisionless magnetoplasma. Laser Part. Beams **28**(2), 343–349 (2010)
14. V. Nanda, N. Kant, M.A. Wani, Self-focusing of a Hermite-cosh Gaussian laser beam in a magnetoplasma with ramp density profile. Phys. Plasmas **20**(11), 4833635 (2013)
15. V. Nanda, N. Kant, Enhanced relativistic self-focusing of Hermite-cosh-Gaussian laser beam in plasma under density transition. Phys. Plasmas **21**(4), 4870080 (2014)
16. S. Kaur et al., Propagation characteristics of Hermite-cosh-Gaussian laser beam in a rippled density plasmas. Laser Part. Beams **35**(1), 100–107 (2017)
17. M.A. Wani, H.S. Ghotra, N. Kant, Self-focusing of Hermite-cosh-Gaussian laser beam in semiconductor quantum plasma. Optik **154**, 497–502 (2018)
18. V. Sharma, V. Thakur, N. Kant, Hermite-cosh-Gaussian laser-induced third harmonic generation in plasma. Opt. Quant. Electron. **53**(6), 281 (2021)
19. A. Varma, A. Kumar, Electron Bernstein wave aided beat wave of Hermite-cosh-Gaussian laser beam absorption in a collisional nanocluster plasma. Optik **245**, 167702 (2021)
20. J. Wadhwa, A. Singh, Generation of second harmonics of intense Hermite-Gaussian laser beam in relativistic plasma. Laser Part. Beams **37**(1), 79–85 (2019)
21. H. Hamster et al., Short-pulse terahertz radiation from high-intensity-laser-produced plasmas. Phys. Rev. E **49**(1), 671 (1994)
22. S. Safari, B. Jazi, About generation of terahertz radiation due to the nonlinear interaction of Gaussian and Hermite–Cosh–Gaussian laser beams in collisional plasma background: Optimization and field profile controlling. IEEE Trans. Plasma Sci. **47**(1), 155–161 (2018)
23. S. Chaudhary et al., Radially polarized terahertz (Terahertz) generation by frequency difference of Hermite Cosh Gaussian lasers in hot electron-collisional plasma. Opt. Lasers Eng. **134**, 106257 (2020)
24. A.K. Malik et al., Terahertz radiation generation by frequency mixing of Hermite–Cosh–Gaussian laser beams in density-modulated cold magnetized plasma. IEEE Trans. Plasma Sci. **49**(9), 3022–3028 (2021)
25. M. Hashemzadeh, Terahertz radiation generation by Hermite-cosh Gaussian and hollow Gaussian laser beams in magnetized inhomogeneous plasmas. Braz. J. Phys. **53**(2), 46 (2023)
26. V. Sharma, V. Thakur, N. Kant, Second harmonic generation of cosh-Gaussian laser beam in magnetized plasma. Opt. Quant. Electron. **52**(10), 444 (2020)
27. S. Safari et al., Terahertz radiation generation through the nonlinear interaction of Hermite and Laguerre Gaussian laser beams with collisional plasma: field profile optimization. J. Appl. Phys. **123**(15), 5019430 (2018)
28. J. Rajput, A.K. Pramanik, P. Kumar et al., Comparative study of electron acceleration by linearly and circularly polarized Hermite-cosh-Gaussian laser pulse in a vacuum. J. Opt. **52**, 642–647 (2023)
29. A. Mehta, J. Rajput, N. Kant, Effect of frequency-chirped laser pulses on terahertz radiation generation in magnetized plasma. Laser Phys. **29**(9), 095405 (2019)
30. A. Mehta et al., Terahertz generation by beating of two chirped pulse lasers in spatially periodic density plasma. Laser Phys. **30**(4), 045402 (2020)
31. X. Wu et al., Highly efficient generation of 0.2 mJ terahertz pulses in lithium niobate at room temperature with sub-50 fs chirped Ti: sapphire laser pulses. Opt. Express **26**(6), 7107–7116 (2018)
32. J. Li et al., Efficient terahertz wave generation from GaP crystals pumped by chirp-controlled pulses from femtosecond photonic crystal fiber amplifier. Appl. Phys. Lett.Lett. **104**(3), 4862270 (2014)
33. M.C. Gurjar et al., High-field coherent terahertz radiation generation from chirped laser pulse interaction with plasmas. IEEE Trans. Plasma Sci. **48**(10), 3727–3734 (2020)
34. V. Thakur, N. Kant, Resonant second harmonic generation in plasma under exponential density ramp profile. Optik **168**, 159–164 (2018)
35. W. Sun, X. Wang, Y. Zhang, Terahertz generation from laser-induced plasma. Opto-Electron. Sci. **1**(8), 220003–220011 (2022)
36. V. Thakur, N. Kant, Optimization of wiggler wave number for density transition based second harmonic generation in laser plasma interaction. Optik **142**, 455–462 (2017)
37. Y. Li et al., High power terahertz pulses generated in intense laser—plasma interactions. Chin. Phys. B **21**(9), 095203 (2012)
38. V. Thakur et al., Influence of exponential density ramp on second harmonic generation by a short pulse laser in magnetized plasma. Optik **171**, 523–528 (2018)
39. G.Q. Liao et al., Intense terahertz radiation from relativistic laser–plasma interactions. Plasma Phys. Controll. Fusion **59**(1), 014039 (2016)
40. V. Thakur, N. Kant, Combined effect of chirp and exponential density ramp on relativistic self-focusing of Hermite-Cosine-Gaussian laser in collisionless cold quantum plasma. Braz. J. Phys. **49**(1), 113–118 (2019)
41. H. Wu et al., Powerful terahertz emission from laser wakefields in inhomogeneous magnetized plasmas. Phys. Rev. E **75**(1), 016407 (2007)

42. V. Thakur, N. Kant, Effect of pulse slippage on density transition-based resonant third-harmonic generation of short-pulse laser in plasma. Front. Phys. **11**, 1–8 (2016)
43. H. Zhong, N. Karpowicz, X.-C. Zhang, Terahertz emission profile from laser-induced air plasma. Appl. Phys. Lett.Lett. **88**(26), 2216025 (2006)